http://www.kidney-international.org

see commentary on page 282

Uremia-related vascular calcification: More than apatite deposition

SC Verberckmoes[1], V Persy[1], GJ Behets[1], E Neven[1], A Hufkens[1], H Zebger-Gong[2], D Müller[2], D Haffner[2,3], U Querfeld[2], S Bohic[4], ME De Broe[1] and PC D'Haese[1]

[1]*Laboratory of Physiopathology, University of Antwerp, Antwerp, Belgium;* [2]*Department of Pediatric Nephrology, Charité Universitätsmedizin Berlin and Center for Cardiovascular Research, Berlin, Germany;* [3]*Department of Pediatrics, University Hospital, Rostock, Germany and* [4]*European Synchrotron Radiation Facility, Grenoble, France*

In the present study, we characterized and compared the mineral phase deposited in the aortic wall of two different frequently used chronic renal failure rat models of vascular calcification. Vascular calcification was induced in rats by either a 4-week adenine treatment followed by a 10-week high-phosphate diet or 5/6 nephrectomy followed by 6 weeks of 0.25 μg/kg/day calcitriol treatment and a high-phosphate diet. Multi-element mapping for calcium and phosphate together with mineral identification was performed on several regions of aortic sections by means of synchrotron X-ray-μ-fluorescence and diffraction. Bulk calcium and magnesium content of the aorta was assessed using flame atomic absorption spectrometry. Based on the diffraction data the Von Kossa-positive precipitate in the aortic regions ($N = 38$) could be classified into three groups: (1) amorphous precipitate (absence of any diffraction peak pattern, $N = 12$); (2) apatite ($N = 16$); (3) a combination of apatite and magnesium-containing whitlockite ($N = 10$). The occurrence of these precipitates differed significantly between the two models. Furthermore, the combination of apatite and whitlockite was exclusively found in the calcitriol-treated animals.

These data indicate that in adenine/phosphate-induced uremia-related vascular calcification, apatite is the main component of the mineral phase. The presence of magnesium-containing whitlockite found in addition to apatite in the vitamin D-treated rats, has to be seen in view of the well-known vitamin D-stimulated gastrointestinal absorption of magnesium.

Kidney International (2007) **71,** 298–303. doi:10.1038/sj.ki.5002028; published online 6 December 2006

KEYWORDS: vitamin D; mineral metabolism; cardiovascular disease; vascular calcification

Correspondence: *PC D'Haese, Department of Physiopathology, University of Antwerp, p/a Antwerp University, Universiteitsplein 1, B-2610 Wilrijk, Belgium. E-mail: patrick.dhaese@ua.ac.be*

Received 17 July 2006; revised 13 September 2006; accepted 18 October 2006; published online 6 December 2006

Cardiovascular events are responsible for almost 50% of the mortality in hemodialysis patients. In patients with chronic kidney disease, vascular disease is often accompanied by arterial calcifications.[1] Several investigators have shown that coronary artery calcifications are already present in young dialysis patients[2,3] tend to progress rapidly[4] and are associated with decreased survival related to the vascular site containing calcifications.[5,6]

Elevated serum phosphate levels, hyperparathyroidism, and an increased Ca × P product are identified as independent risk factors for coronary artery calcifications.[2,4] Treatment of secondary hyperparathyroidism with calcitriol is currently recommended in adult and pediatric patients with chronic kidney disease.[7,8] However, the suppressive effect of calcitriol on parathyroid hormone release goes along with an increased calcium/phosphorus gastrointestinal absorption, favoring ectopic calcification.

Vascular calcification is a tightly regulated process driven by specific cellular events[9,10] and particular components present in the serum.[11] Transdifferentiation of vascular smooth muscle cells towards cells with an osteogenic phenotype, expressing the major bone-specific proteins, is a key event in the process of medial calcification.[12] Based on these observations it is generally assumed that the mineral deposited in the vascular wall has the physicochemical properties of hydroxyapatite, the mineral compound of bone. However, owing to the limited availability of appropriate techniques data on the identity and ultrastructural composition of the mineral phase deposited during vascular calcification are scarce.[13,14]

By the application of synchrotron radiation based X-ray μ-fluorescence in combination with μ-diffraction analysis, we studied the ultrastructural spatial composition of the mineral deposited in the vessel wall of calcitriol- and non-calcitriol-treated models of uremia-induced vascular calcification.

RESULTS

Both rat models, that is, the combination of (i) adenine treatment with a high-phosphate diet and (ii) 5/6 nephrectomy, a high-phosphate diet, and oral dosing of calcitriol

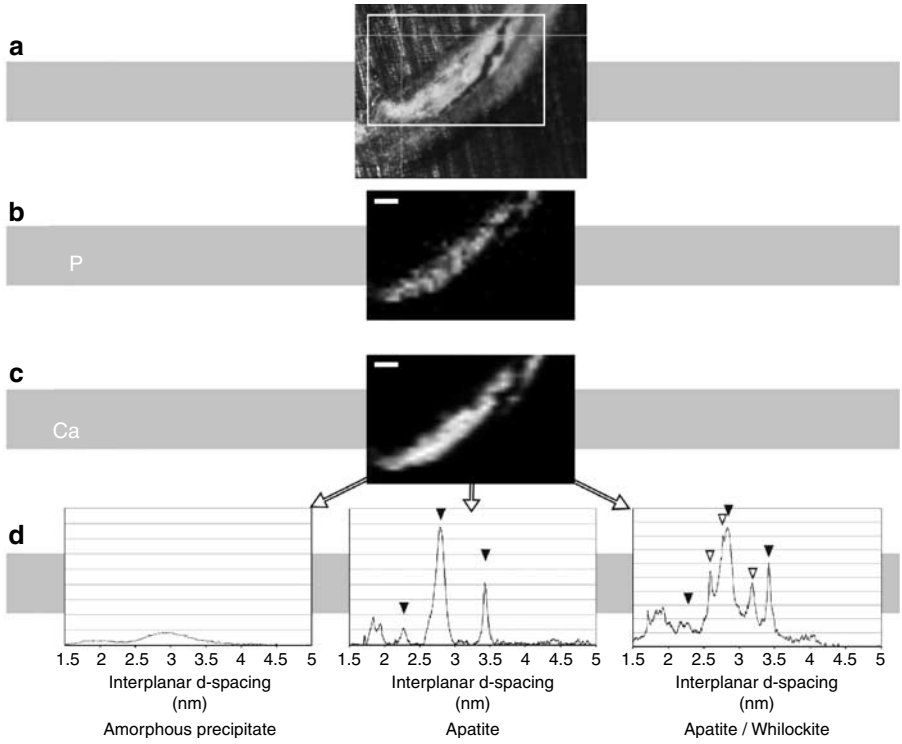

Figure 1 | Mineral identification in the calcified aorta of uremic rats. (**a**) Based on a video microscopic image of the aortic wall a region of interest was defined which was further investigated by means of X-ray fluorescence mapping for the presence of (**b**) phosphorus and (**c**) calcium (Bar = 50 μm). By performing several line scans through the region of interest X-ray diffraction patterns were recorded and averaged over the line scan. (**d**) After the circular integration of the recorded diffraction patterns (see Materials and Methods) the mineral phase of the investigated aortic region could be identified either as (i) amorphous precipitate, (ii) apatite, or (iii) a mixture of apatite and whitlockite. In some aortic regions the calcium phosphate was present as an amorphous precipitate whereas in others the mineral could be identified as calcium apatite (black arrow heads). Only samples originating from the vitamin D-treated renal failure animals next to apatite (black arrow heads) also an additional mineral phase was found, identified as whitlockite (open arrow heads).

resulted in mineral deposition in the vascular wall, as could be visualized by Von Kossa staining (data not shown).[15,16]

X-ray-μ-fluorescence analysis was performed on aorta samples obtained from rats of both models with a positive Von Kossa staining. In all investigated microscopic aortic regions of interest ($N = 38$) a positive X-ray fluorescence signal for phosphorus and calcium was observed (Figure 1b and c). By recording the X-ray diffraction patterns of several calcium- and phosphorus-positive spots in the investigated aortic regions three different types of mineral were identified (Table 1): (i) amorphous calcium phosphate precipitate in the absence of any diffraction peak pattern ($N = 12$), or (ii) poorly crystalline apatite (microcrystalline or non-stoechiometric apatite) ($N = 16$), or (iii) a combination of apatite and whitlockite ($N = 10$) (Figure 1d). The occurrence of the various types significantly ($P < 0.05$) differed between the two models and the combination of apatite and whitlockite mineral was exclusively found in vitamin D-treated animals (Table 1).

The spatial heterogeneity of the apatite and apatite/whitlockite mineral deposition in the aorta was further investigated by performing 10 μm step size line scans through the vascular wall. At each point, the calcium fluorescence (Figure 2, upper panels) and diffraction pattern (Figure 2, lower panels) were recorded simultaneously. In all samples positive for poorly crystalline apatite or a combination of apatite and whitlockite, amorphous precipitate was found at the edges of the calcified region (upper panels of Figure 2a and b, shaded zone) as indicated by a positive calcium signal in the absence of a diffraction pattern (Figure 1d). Moreover, in samples where the mineral was identified as a mixture of whitlockite and apatite, the fluorescence/diffraction line scan analysis showed areas positive (Figure 2b, left diffraction pattern) and negative (Figure 2b, right diffraction pattern) for the presence of whitlockite indicating a heterogenic distribution of this mineral phase in the vessel wall of calcitriol-treated animals.

Table 1 | Distribution of the different mineral phases in the investigated aortic regions

	Amorphous precipitate	Apatite	Apatite/ whitlockite
Adenine model	1	7	0
Calcitriol-treated remnant kidney model	11	9	10

χ^2 analysis revealed significant proportional differences (P=0.012) in the occurrence of the mineral phases between the two rat models.

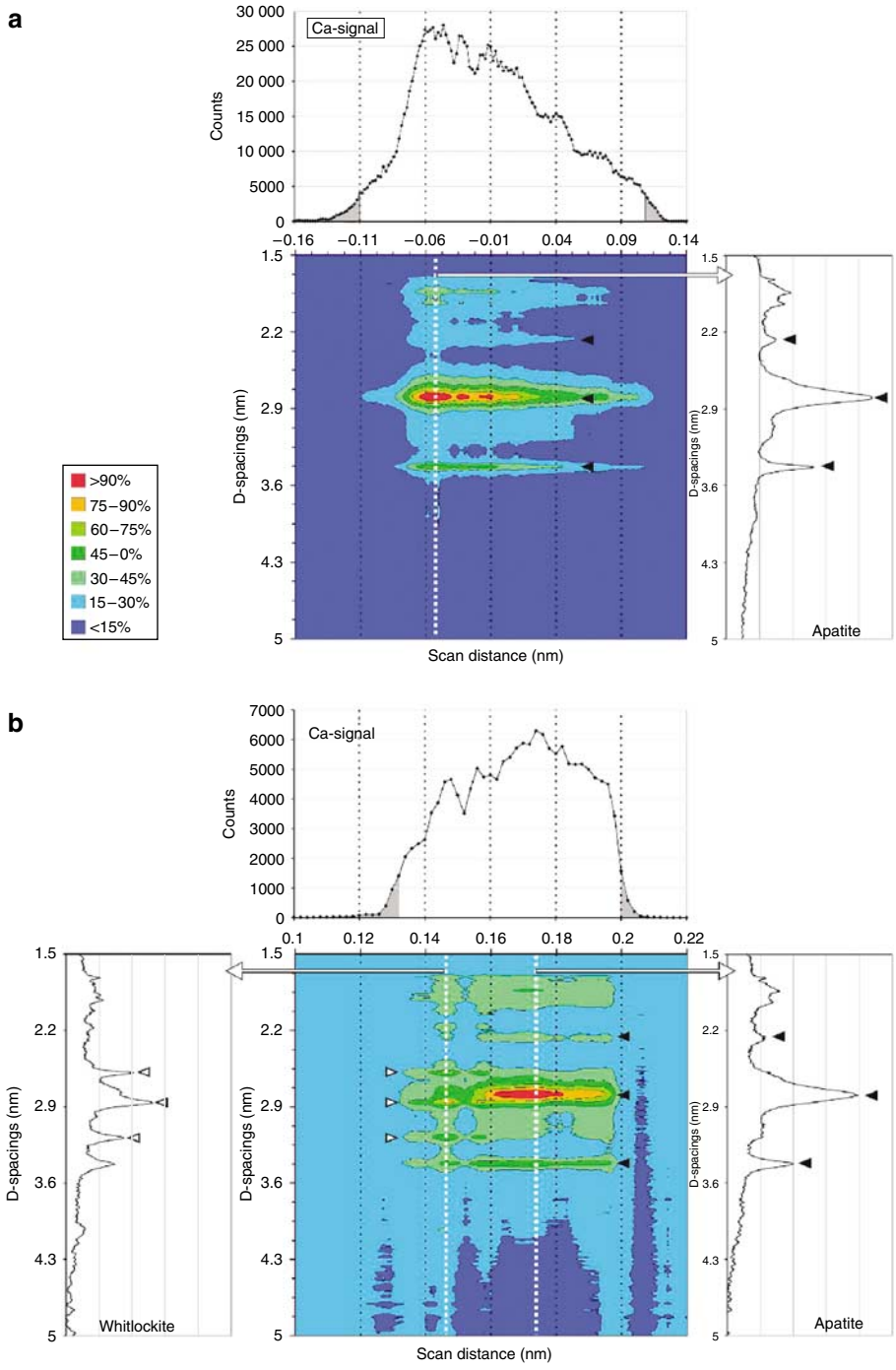

Figure 2 | Calcium X-ray fluorescence and X-ray diffraction patterns of the deposited mineral in the aorta of uremic rats. Representation of the ultrastructural spatial heterogeneity of the identified mineral phases: (a) apatite and (b) apatite and whitlockite. These mineral phases were further investigated by performing line scans with a 10 μm step size through the vessel wall. During this line scan patterns both X-ray fluorescence for calcium (upper panel) and diffraction (lower panel) were recorded for each 10 μm step. The integrated diffraction pattern for each point of the line scan is presented in the lower panel as percentage of maximum peak intensity in a 2D-height-field. The gray shaded regions in the calcium signal in the upper panel for (**a**) apatite and (**b**) apatite and whitlockite represent the scan points where no mineral phase but amorphous calcium phosphate phase was found. The white dotted line through the diffraction height-field marks the position of the detailed diffraction patterns shown left (whitlockite) and right (apatite). The white arrow heads indicate the diffraction peak positions typical for whitlockite whereas the black arrow heads indicate the apatite peaks. These data also show that the whitlockite mineral phase is not homogeneously distributed through the aortic calcification.

As the formation of whitlockite has been associated with the presence of magnesium,[17,18] serum and mineralized aortas of both models were analyzed for their calcium and magnesium content. No difference in serum magnesium concentration was found (0.037 ± 0.019 vs 0.032 ± 0.019 μg/ml magnesium in adenine treated vs calcitriol treated 5/6

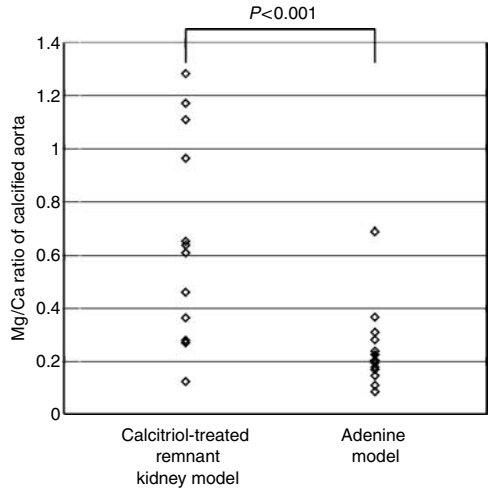

Figure 3 | Magnesium/calcium ratios of the calcified aortas in both models. Statistical evaluation of the data with a Mann–Whitney test showed a significantly ($P<0.05$) higher magnesium/calcium ratio in the aortas of vitamin D-treated 5/6 nephrectomized rats vs adenine-treated animals receiving a high-phosphate diet.

nephrectomized rats, respectively). In contrast, the calcified areas of the aorta obtained from subtotally nephrectomized animals loaded with calcitriol showed a significantly ($P<0.001$) higher magnesium/calcium ratio compared to rats with adenine-induced renal failure receiving a high-phosphate diet (median: 0.63, range: 0.12–1.28 (mean $\pm$ s.d.: 0.48 ± 0.23) vs median: 0.22, range: 0.09–0.69 (mean $\pm$ s.d.: 0.32 ± 0.18); Figure 3).

DISCUSSION

Recent *in vitro* studies have shown that vascular calcification is a tightly regulated process in which the vascular smooth muscle cell undergoes a trans-differentiation towards an osteogenic phenotype.[12] *In vitro* data further suggest that the mineral compound present in the vascular wall is microcrystalline apatite,[9,13,19] as it naturally occurs in bone. Indeed, the presence of hydroxyapatite in the aorta of uremic rats was suggested as early as 1979 by the application of X-ray fluorescence micro analysis.[20] This technique, however, only provides information concerning the elemental composition, and does not allow the identification of the mineral phase. In an autopsy study of patients with end-stage renal disease, hydroxyapatite and calcium phosphate were found in calcified atherosclerotic plaques by the application of X-ray diffraction.[21] Although these observations[20,22] have provided valuable information on the nature of severe atherosclerotic lesions, much less is known of the physicochemical properties of mineral deposits in the vascular media in uremia. Such information might further contribute to the unraveling of the mechanisms leading to the formation/possible reversal of vascular calcification in renal disease.

In the present study, two frequently used models of uremia-related vascular calcification were compared at the level of deposited mineral. Interestingly, between the investigated models a significantly difference in distribution of mineral phases (both amorphous calcium phosphate and whitlockite) was found.

Calcium phosphate precipitating from a supersaturated solution *in vitro* is initially an amorphous compound which is converted into the thermodynamically more stable microcrystalline apatite form.[17] This process occurs also in biological mineralization such as in bone formation.[23,24] Hence, in the frame of the current study it is not surprising that both amorphous calcium phosphate and poorly crystalline apatite were present in the calcified aorta of uremic rats exposed to either calcitriol and/or a high-phosphate diet. The application of synchrotron X-ray-μ-diffraction with an X-ray probe size of $2 \times 10\,\mu$m enabled us to study the spatial heterogeneity of the mineral phase in the vascular media at the ultrastructural micrometer-scale level. This evaluation showed the presence of amorphous calcium phosphate at the edges of the mineral phases. This observation fits well with previous findings in that the amorphous calcium phosphate precipitate is an early deposit which matures over time under the formation of calcium apatite.[17] Moreover, as amorphous calcium phosphate is a labile precipitate its presence suggests that the mineral deposition in vascular calcification may be reversible at these sites.

Surprisingly, in 1/3 of the aortic regions of animals exposed to calcitriol, the mineral phase consisted not only of apatite but contained also whitlockite, which is a calcium-magnesium orthophosphate, that is, $(Ca,Mg)_3(PO_4)_2$.[18,17] Already at low concentrations, magnesium ions have a marked effect on nucleation and growth of calcium phosphates. These ions delay the conversion of amorphous calcium precipitates to the more stable apatite phase and promote the formation of whitlockite.[17,18,25] As (i) X-ray diffraction only offers information on mineral lattice characteristics, but not of the mineral composition, and (ii) the applied X-ray-μ-fluorescence technique was not suitable to detect chemical elements with low atomic number, such as magnesium, flame atomic absorption spectroscopy was used to determine the bulk magnesium content in calcified aortas of both models of vascular calcification. The presence of a significantly higher magnesium/calcium ratio in the aortas of calcitriol-treated animals vs the adenine-treated rats strongly supports the presence of whitlockite. These new findings are in line with previous observations showing that calcitriol supplementation not only stimulates calcium and phosphorus uptake but also favors the gastrointestinal absorption of magnesium.[26,27] As under normal physiological conditions the kidney plays a central role in the metabolism of magnesium it is not surprising that magnesium accumulation occurs in the presence of renal failure.[28]

The observed difference in mineral composition between the two investigated models of uremia-related vascular calcification cannot be ascribed to the methodology applied inducing chronic renal failure as the degree of renal impairment and other biochemical parameters ($Ca \times P$ product and parathyroid hormone) were comparable. The only significant difference between both models was the duration of uremia,

with a three weeks longer period in renal insufficiency in the adenine-treated rats. This has the consequence that the deposited precipitate in the adenine-treated rats had a longer maturation time. This, together with the possible effects of magnesium delaying the formation of stable apatite in the calcitriol-treated animals can explain the difference in distribution of the amorphous phase between both models.

Recently, a link between the status of bone metabolism and vascular calcification has been made.[29] In this context it has to be noted that it has been reported that adenine treatment not only induces chronic renal failure but also affects steroidogenesis and reduces bone metabolism resulting in a reduced bone mineral density.[30] Although the male gender and a reduced bone mineral density have been considered as risk factors for the development of vascular calcification, such an effect can be excluded as histomorphometric analysis of bone samples of the adenine-treated animals did not show a reduced bone area or signs of a reduced bone mineral density. Instead a histological picture of secondary hyperparathyroidism was found (Persy *et al*. SA-PoO950, ASN, Renal Week 2004). Because of the high-phosphate diet in combination with the severe renal failure, the vitamin D-treated animals also showed the histological features of secondary hyperparathyroidism.

The physiopathological role and clinical importance of whitlockite is much less studied compared to apatite and its relevance may have been largely underestimated as the classical Von Kossa staining for calcified tissues does not allow to differentiate between whitlockite and apatite. Techniques such as X-ray or electron diffraction and infrared spectrometry that allow discrimination between mineral phases are not routinely applied on biological/pathological samples. To the best of our knowledge only one publication is available in literature that mentions the presence of whitlockite in the vascular media of autopsy samples of subjects of the general population.[31] In contrast with our findings, however, in the latter paper no microanalysis was performed, nor was the heterogeneity of the mineral phase investigated. Moreover, the occurrence of whitlockite in arterial calcifications in uremic patients and its association with calcitriol treatment has not been described previously. Our results indicate that the process of uremia-related vascular calcification is not solely owing to the deposition of calcium-apatite and that a role for magnesium in the pathogenesis of uremia-related calcification should be considered – especially during calcitriol treatment.

MATERIALS AND METHODS

This study was performed as an extension of two previous studies on either the effect of adenine treatment and a high-phosphate diet[16] or a 5/6 nephrectomy and calcitriol-treatment[15] on the induction of vascular calcification.

Animal models

Medical vascular calcifications were induced in two models of chronic renal failure.

Adenine model of chronic renal failure. Chronic renal failure was induced by feeding male Wistar rats a diet containing 0.75%. adenine and 0.92% phosphorus for 4 weeks, which has been shown to induce a stable, moderate to severe renal function impairment.[32] Following adenine treatment the animals ($N = 13$) were fed a diet containing 1.06% calcium and 1.03% phosphorus during 6 weeks until killing.[16]

Remnant kidney model of chronic renal failure. Male Sprague–Dawley rats underwent a 5/6 nephrectomy to induce chronic renal failure. Two days after surgery (day 0), the animals received 0.25 μg/kg. of $1,25(OH)_2D_3$ (Rocaltrol™, Roche, Mannheim, Germany) postoperatively daily for 6 weeks. Animals ($N = 12$) received a standard commercial diet containing 1.2% phosphorus, 0.9% calcium (Altromin™, Altromin Co., Lage, Germany).[15]

Sample preparation

Through a combined midline laparotomy and thoracotomy the vascular tree was exposed and the large vessels were removed '*en bloc*'. The aorta was divided in different pieces; one piece was used for general histology after paraffin embedding, another was embedded with methyl methacrylate for mineral identification, whereas a third part was used for bulk analysis.

Methyl methacrylate embedding of the aorta samples was performed using a standard procedure as reported elsewhere.[33] A 10-μm thick methyl methacrylate-embedded aorta section was used for evaluation of the mineral deposition in the vessel wall by Von Kossa staining and counterstaining with hematoxylin and eosin. Another 10 μm section (adjacent to the Von Kossa-stained section) was dried unstained between two glass cover slides at 60°C, and used for synchrotron X-ray-μ-fluorescence and X-ray-μ-diffraction analysis.

Analysis of serum and bulk tissue calcium and magnesium content

Unfixed tissue samples were weighed with a precision balance and subsequently digested in 65% nitric acid at 65°C overnight. Serum and tissue calcium and magnesium content was measured by flame atomic absorption spectrometry (Model 3110, Perkin-Elmer, Norwalk, CT, USA) after appropriate further dilution of the samples in 0.1% lanthanum nitrate to avoid chemical interferences.

Mineral identification

Unstained 10-μm thick methyl methacrylate-embedded aorta sections adjacent to those stained positive for Von Kossa were investigated by X-ray-μ-analysis. Several regions of interest were defined on each sample which were investigated by synchrotron X-ray-μ-fluorescence and X-ray-μ-diffraction on beam line ID18F of the European Synchrotron Radiation Facility (Grenoble, France)[34] applying a same beamline set-up as published before.[35] The optimum step-size for either raster or line scans is determined by the size of the focused beam (2×10 μm) and was set to 10 μm in both directions (horizontally and vertically). Calcium and phosphorus mapping were obtained by integrating the fluorescence intensities defined by the appropriate energy windows for the respective element (calcium: 3.47–4.24 keV and phosphorus: 1.81–2.13 keV) during a recording time of 1 s.

Integration of the obtained circular X-ray-μ-diffraction patterns to d-spacing format (d = interplanar or interatomic distance) was carried out using the X-ray diffraction software package FIT2D

developed by Hammersley *et al.*[36] Comparison with the reference diffraction spectra for synthetic hydroxyapatite ($Ca_{10}(PO_4)_6(OH)_2$: PDF #86-0740) and whitlockite ($(Ca,Mg)_3(PO_4)_2$: PDF #70-2064) from the powder diffraction database PCPDFWIN version 2.1 (International Centre of Diffraction Data, USA) was performed after background correction of the integrated X-ray diffraction spectra.

Statistics

Results of the bulk analysis of the magnesium/calcium ratio in the rat aorta were analyzed for significant differences using the non-parametric Mann–Whitney test. Comparison of the prevalence of the various mineral phases in the two models was carried out by χ^2 analysis. *P*-values <0.05 (two tailed) were considered as significant.

ACKNOWLEDGMENTS

We acknowledge the European Synchrotron Radiation Facility for provision of synchrotron radiation facilities and for assistance in using beamline ID18F.

REFERENCES

1. Foley RN, Parfrey PS, Sarnak MJ. Epidemiology of cardiovascular disease in chronic renal disease. *J Am Soc Nephrol* 1998; **9**(12 Suppl): S16–S23.
2. Oh J, Wunsch R, Turzer M *et al.* Advanced coronary and carotid arteriopathy in young adults with childhood-onset chronic renal failure. *Circulation* 2002; **106**: 100–105.
3. Eifinger F, Wahn F, Querfeld U *et al.* Coronary artery calcifications in children and young adults treated with renal replacement therapy. *Nephrol Dial Transplant* 2000; **15**: 1892–1894.
4. Goodman WG, Goldin J, Kuizon BD *et al.* Coronary-artery calcification in young adults with end-stage renal disease who are undergoing dialysis. *N Engl J Med* 2000; **342**: 1478–1483.
5. London GM, Pannier B, Guerin AP *et al.* Alterations of left ventricular hypertrophy in and survival of patients receiving hemodialysis: follow-up of an interventional study. *J Am Soc Nephrol* 2001; **12**: 2759–2767.
6. Blacher J, Guerin AP, Pannier B *et al.* Arterial calcifications, arterial stiffness, and cardiovascular risk in end-stage renal disease. *Hypertension* 2001; **38**: 938–942.
7. Eknoyan G, Levin A, Levin NW. K/DOQI clinical practice guidelines for bone metabolism and disease in chronic kidney disease – foreword. *Am J Kidney Dis* 2003; **42**: S7–S201.
8. Klaus G, Watson A, Edefonti A *et al.* Prevention and treatment of renal osteodystrophy in children on chronic renal failure: European guidelines. *Pediatr Nephrol* 2006; **21**: 151–159.
9. Reynolds JL, Joannides AJ, Skepper JN *et al.* Human vascular smooth muscle cells undergo vesicle-mediated calcification in response to changes in extracellular calcium and phosphate concentrations: a potential mechanism for accelerated vascular calcification in ESRD. *J Am Soc Nephrol* 2004; **15**: 2857–2867.
10. Chen NX, O'Neill KD, Duan D *et al.* Phosphorus and uremic serum up-regulate osteopontin expression in vascular smooth muscle cells. *Kidney Int* 2002; **62**: 1724–1731.
11. Ketteler M, Gross ML, Ritz E. Calcification and cardiovascular problems in renal failure. *Kidney Int* 2005; **67**(Suppl 94): S120–S127.
12. Yang H, Curinga G, Giachelli CM. Elevated extracellular calcium levels induce smooth muscle cell matrix mineralization *in vitro*. *Kidney Int* 2004; **66**: 2293–2299.
13. Lomashvili KA, Cobbs S, Hennigar RA *et al.* Phosphate-induced vascular calcification: role of pyrophosphate and osteopontin. *J Am Soc Nephrol* 2004; **15**: 1392–1401.
14. LeGeros RZ. Formation and transformation of calcium phosphates: relevance to vascular calcification. *Z Kardiol* 2001; **90**(Suppl 3): 116–124.
15. Haffner D, Hocher B, Muller D *et al.* Systemic cardiovascular disease in uremic rats induced by $1,25(OH)_2D_3$. *J Hypertens* 2005; **23**: 1067–1075.
16. Persy VP, Postnov A, Neven E *et al.* Detection of vascular calcifications by high resolution X-ray microtomography in living rats with chronic renal failure. *Arterioscler Thromb Vasc Biol* 2006; **26**: 2110–2116.
17. Hamad M, Heughebaert J. The growth of whitlockite. *J Crystal Growth* 1986; **79**: 192–197.
18. Lagier R, Baud CA. Magnesium whitlockite, a calcium phosphate crystal of special interest in pathology. *Pathol Res Pract* 2003; **199**: 329–335.
19. Moe SM, Duan D, Doehle BP *et al.* Uremia induces the osteoblast differentiation factor Cbfa1 in human blood vessels. *Kidney Int* 2003; **63**: 1003–1011.
20. Ejerblad S, Ericsson JL. Ultrastructure of the aorta in experimental uraemia. *Acta Chir Scand* 1979; **145**: 331–343.
21. Schwarz U, Buzello M, Ritz E *et al.* Morphology of coronary atherosclerotic lesions in patients with end-stage renal failure. *Nephrol Dial Transplant* 2000; **15**: 218–223.
22. Massy ZA, Ivanovski O, Nguyen-Khoa T *et al.* Uremia accelerates both atherosclerosis and arterial calcification in apolipoprotein E knockout mice. *J Am Soc Nephrol* 2005; **16**: 109–116.
23. Rey C, Hina A, Tofighi A *et al.* Maturation of poorly crystalline apatites: chemical and structural aspects *in vivo* and *in vitro*. *Cells Mater* 1995; **5**: 345–356.
24. Rey C, Shimizu M, Collins B *et al.* Resolution-enhanced Fourier transform infrared spectroscopy study of the environment of phosphate ion in the early deposits of a solid phase of calcium phosphate in bone and enamel and their evolution with age: 2. Investigations in the nu3PO4 domain. *Calcif Tissue Int* 1991; **49**: 383–388.
25. Ennever J, Vogel JJ. Magnesium inhibition of apatite nucleation by proteolipid. *J Dent Res* 1981; **60**: 838–841.
26. Hardwick LL, Jones MR, Brautbar N *et al.* Magnesium absorption: mechanisms and the influence of vitamin D, calcium and phosphate. *J Nutr* 1991; **121**: 13–23.
27. Schweigel M, Martens H. Magnesium transport in the gastrointestinal tract. *Front Biosci* 2000; **5**: D666–D677.
28. Lindeman RD. Chronic renal failure and magnesium metabolism. *Magnesium* 1986; **5**: 293–300.
29. Moe SM. Vascular calcification and renal osteodystrophy relationship in chronic kidney disease. *Eur J Clin Invest* 2006; **36**(Suppl 2): 51–62.
30. Ogirima T, Tano K, Kanehara M *et al.* Sex difference of adenine effects in rats: renal function, bone mineral density and sex steroidogenesis. *Endocr J* 2006; **53**: 407–413.
31. Reid JD, Andersen ME. Medial calcification (whitlockite) in the aorta. *Atherosclerosis* 1993; **101**: 213–224.
32. Okada H, Kaneko Y, Yawata T *et al.* Reversibility of adenine-induced renal failure in rats. *Clin Exp Immunol* 2005; **3**: 82–88.
33. Behets GJ, Dams G, Damment S *et al.* An assessment of the effects of lanthanum on bone in a chronic renal failure (CRF) rat model. *J Am Soc Nephrol* 2001; **12**: 740A.
34. Vekemans B, Vincze L, Somogyi A *et al.* Quantitative X-ray fluorescence analysis at the ESRF ID18F microprobe. *Nuclear Instruments & Methods in Physics Research Section B-Beam Interactions with Materials and Atoms* 2003; **199**: 369–401.
35. Verberckmoes SC, Behets GJ, Oste L *et al.* Effects of strontium on the physicochemical characteristics of hydroxyapatite. *Calcif Tissue Int* 2004; **75**: 405–415.
36. Hammersley AP, Svensson SO, Hanfland M *et al.* Two-dimensional detector software: from real detector to idealised image or two-theta scan. *High Press Res* 1996; **14**: 235–248.